Parallel Evaluation of Alternative Skin Barrier Models and Excised Human Skin for Dermal Absorption Studies In Vitro

Alec T. Salminen[1], **Kelly J. Davis**[2], **Robert P. Felton**[3], **Nathania Nischal**[1], **Linda S. VonTungeln**[1], **Frederick A. Beland**[1], **Kristy Derr**[4], **Paul C. Brown**[5], **Marc Ferrer**[4], **Linda M. Katz**[6], **Nicole C. Kleinstreuer**[7], **Jonathan Leshin**[8], **Prashiela Manga**[6], **Nakissa Sadrieh**[5], **Menghang Xia**[4], **Suzanne C. Fitzpatrick**[6], **Luísa Camacho**[1,*]

[1]Division of Biochemical Toxicology, National Center for Toxicological Research, U.S. Food and Drug Administration, Jefferson, AR, USA

[2]Toxicologic Pathology Associates, Jefferson, AR, USA

[3]Office of Scientific Coordination, National Center for Toxicological Research, U.S. Food and Drug Administration, Jefferson, AR, USA

[4]National Center for Advancing Translational Sciences, National Institutes of Health, Rockville, MD, USA

[5]Center for Drug Evaluation and Research, U.S. Food and Drug Administration, Silver Spring, MD, USA

*Corresponding author: Luísa Camacho, Luisa.Camacho@fda.hhs.gov, Telephone: +1 (870) 543-7588, Address: National Center for Toxicological Research, Food and Drug Administration, 3900 NCTR Rd, Jefferson, AR 72079.

[6]CRediT Author Statement

ATS: Conceptualization, Methodology, Investigation, Visualization, Writing – Original Draft
KJD: Methodology, Investigation, Writing – Review & Editing
RPF: Formal Analysis, Writing – Review & Editing
NN: Investigation, Writing – Review & Editing
LSV: Methodology, Writing – Review & Editing
FAB: Resources, Writing – Review & Editing
KD: Methodology, Writing – Review & Editing
PCB: Conceptualization, Writing – Review & Editing
MF: Conceptualization, Writing – Review & Editing
LMK: Conceptualization, Writing – Review & Editing
NCK: Conceptualization, Writing – Review & Editing
JL: Conceptualization, Writing – Review & Editing
PM: Conceptualization, Writing – Review & Editing
NS: Conceptualization, Writing – Review & Editing
MX: Conceptualization, Writing – Review & Editing
SCF: Conceptualization, Writing – Review & Editing
LC: Supervision, Conceptualization, Methodology, Investigation, Validation, Funding acquisition, Writing – Review & Editing

[9]Disclaimer

This article reflects the views of the authors and does not necessarily reflect those of the U.S. Food and Drug Administration. Any mention of commercial products is for clarification only and is not intended as approval, endorsement, or recommendation.

[10]Supplementary Material

A supplemental file with additional figures and tables and an excel file containing the raw in vitro permeation data are provided.

[6]Center for Food Safety and Applied Nutrition, U.S. Food and Drug Administration, College Park, MD, USA

[7]National Toxicology Program Interagency Center for the Evaluation of Alternative Toxicological Methods, National Institute of Environmental Health Sciences, RTP, NC, USA

[8]Center for Veterinary Medicine, U.S. Food and Drug Administration, Rockville, MD, USA

Abstract

Skin permeation is a primary consideration in the safety assessment of cosmetic ingredients, topical drugs, and human users handling veterinary medicinal products. While excised human skin (EHS) remains the 'gold standard' for in vitro permeation testing (IVPT) studies, unreliable supply and high cost motivate the search for alternative skin barrier models. In this study, a standardized dermal absorption testing protocol was developed to evaluate the suitability of alternative skin barrier models to predict skin absorption in humans. Under this protocol, side-by-side assessments of a commercially available reconstructed human epidermis (RhE) model (EpiDerm-200-X, MatTek), a synthetic barrier membrane (Strat-M, Sigma-Aldrich), and EHS were performed. The skin barrier models were mounted on Franz diffusion cells and the permeation of caffeine, salicylic acid, and testosterone, was quantified. Transepidermal water loss (TEWL) and histology of the biological models were also compared. EpiDerm-200-X exhibited native human epidermis-like morphology, including a characteristic *stratum corneum*, but had an elevated TEWL as compared to EHS. The mean 6 h cumulative permeation of a finite dose (6 nmol/cm^2) of caffeine and testosterone was highest in EpiDerm-200-X, followed by EHS and Strat-M. Salicylic acid permeated most in EHS, followed by EpiDerm-200-X and Strat-M. Overall, evaluating novel alternative skin barrier models in the manner outlined herein has the potential to reduce the time from basic science discovery to regulatory impact.

Keywords

Human Skin; Dermal Absorption; Reconstructed Human Epidermis; In Vitro Permeation Testing; Franz Cell; Strat-M

2   Introduction

Skin is the largest organ of the human body, with a typical surface area of 1.8 m^2 in adults and accounting for around 15% of total adult body weight [1]. Skin performs many vital functions, including thermoregulation, water retention, sensory feedback, metabolism, and protection from external insult [2]. Furthermore, skin is a dynamic organ, continuously shedding and replacing cells to maintain a consistent physiology. Critically, this continuous barrier strictly regulates the transport of numerous biological, chemical, and physical agents to which it is exposed.

Human skin comprises three main layers: the epidermis, the dermis, and the hypodermis [1]. The innermost layer of the skin, the hypodermis (subcutaneous tissue), is a highly vascularized tissue composed of adipocytes, fibroblasts, and macrophages. The middle layer, the dermis, is a fibrous connective tissue composed primarily of collagens (type I and II)

and elastin, providing structural elasticity and rigidity to the skin. Like the hypodermis, the dermis is host to a number of cell types, including cells of the nerve and vascular networks, macrophages, dendritic cells, mast cells, lymphocytes, adipocytes, and most abundantly, fibroblasts/fibrocytes. In addition to protection from physical insult, the dermis plays important sensory feedback and thermoregulation roles. The outermost layer of the skin, the epidermis, is a stratified, squamous epithelium, comprising keratinocytes (~80% of total cells) as well as melanocytes, Langerhans cells, and Merkel cells, and is host to appendages, such as sweat glands and hair follicles. Keratinocytes of the epidermis are organized into four layers depending on morphology and contents, including a basal cell layer (*stratum basale*), a squamous layer (*stratum spinosum*), a granular layer (*stratum granulosum*), and a cornified layer (*stratum corneum*). The basal keratinocytes of the *stratum basale* are polarized epithelial cells that continuously regenerate to supply the subsequent outer epidermal layers [3]. Polarization and plasticity are maintained in part through interactions between the keratinocytes and the basement membrane at the dermo-epidermal junction [4]. As these cells proliferate and migrate to the skin surface, they undergo a terminal differentiation process that involves keratinization, loss of organelles, and cell death, resulting in the formation of corneocytes. These corneocytes, together with a rich intercellular lipid matrix and proteome, make up the *stratum corneum* [5]. The acidic nature of this layer, lack of viable cells, and continuous shedding all contribute to its ability to effectively limit pathogenic microorganism colonization and infection [6]. Critically, given the tortuous pathways between lipids of this layer, the *stratum corneum* is considered the major constituent of the skin barrier [7].

As the skin is continuously exposed to many agents, understanding the ability of such agents to penetrate the skin barrier is a major factor in risk assessment. Whether exposure occurs intentionally (e.g., topical drugs or cosmetics) or unintentionally (e.g., environmental or occupational), it is critical to know the extent to which certain chemicals may penetrate the skin and potentially become systemically available. This information can in turn be used to determine acceptable and/or effective levels of exposure, as well as in risk assessment in which potential harm due to systemic exposure may be identified [8].

Dermal absorption, or the amount of chemical penetrated through the skin, can be estimated through a variety of methods. In vivo human studies can include tape stripping, in which layers of a drug-exposed *stratum corneum* are sequentially removed and analyzed to predict the permeation profile, and dermal microdialysis, in which a probe is inserted into the skin where it can determine the amount of chemical permeated [9]. In vivo animal studies (most notably involving rats and pigs) may also be performed to predict dermal absorption. In such work, skin is topically exposed and excreta, blood, and/or tissues are collected for analysis [10]. Similar studies may be performed in humans, in which skin is topically exposed for a set time, and urine and/or blood is collected at predetermined time points [11].

As the interest in performing dermal absorption studies grows, so does the push to limit the reliance on animal studies in regulatory research [12]. Worldwide, including in the USA, regulatory agencies are invested in reducing, refining, and replacing (3Rs) the use of animals in research. In the study of dermal absorption, this focus has been highlighted by the increased adoption of in vitro methods. Dermal absorption in vitro is determined through

a method termed in vitro permeation testing (IVPT). IVPT involves the use of a diffusion cell, on which excised skin can be mounted and maintained at a physiological temperature and humidity [13]. A common diffusion cell used for such work is the Franz diffusion cell [14, 15]. The Franz cell (FC) is a static vertical diffusion cell composed of receptor and donor chambers, between which skin is mounted. These diffusion cells may also include a chamber surrounding the receptor compartment to function as a water jacket for temperature maintenance, as well as a sample port for continuous access to the receptor compartment fluid. While many skin types have been used to date for IVPT, including porcine, rat, and guinea pig, excised human skin (EHS) is considered the 'gold standard' for in vitro dermal absorption studies [16]. A previous report by Lehman and colleagues [17] comparing existing in vitro and in vivo human percutaneous absorption data found that data obtained from the EHS model correlated well with that obtained in human subjects, particularly when experimental parameters (e.g., anatomical site, vehicle, dose, duration) were harmonized. Of note, the Organization for Economic Co-operation and Development (OECD) provides detailed guidance documents for performing both in vivo and in vitro dermal absorption studies (See OECD Test Guidelines No. 427 and 428, and Guidance Document No. 156).

EHS for IVPT is often obtained from elective surgery. As a result, these tissues are limited in supply, susceptible to donor-dependent variabilities (e.g., due to age, race, sex, disease status, or anatomical region of collection) [18], and associated with high costs. As the demand for EHS increases, it has become apparent that human-relevant alternatives for IVPT are needed if such studies are to be adopted for large scale regulatory work [19]. Various alternative skin barrier models, including synthetic membranes [20, 21], full-thickness human skin equivalents (FTSE) [22, 23], and reconstructed human epidermis (RhE) models [16], have been developed in recent years with potential to aid in the study of dermal absorption; however, a consistent and systematic evaluation of such models for this application is limited. Further, towards regulatory adoption and implementation, standardizing the integration of alternative skin barrier models into established dermal absorption methods is needed.

In this work, we present an approach to evaluate alternative skin barrier models for dermal absorption studies. IVPT parameters were first optimized to ensure broad adaptability of existing and future alternative skin barrier models. Next, these refined methods were implemented to assess the potential of representative alternative skin barrier models to differentiate dermal absorption outcomes depending on the chemical and vehicle used. Ultimately, we found that the RhE model (EpiDerm-200-X) and the synthetic barrier membrane (Strat-M) used here differ greatly in their ability to model compound permeation through EHS. As such, alternative skin barrier models need continued improvement if they are to recapitulate the intricate human skin barrier. Nonetheless, the methods outlined here are expected to permit rapid assessment of novel alternative skin barrier models as they become available, while also determining what aspects of dermal absorption studies are best addressed by various in vitro models. This, in turn, should greatly improve the pipeline from innovation to regulatory toolbox in the context of IVPT.

3 Materials and Methods

3.1 Radioisotopes and Chemicals

Radiolabeled test chemical information can be found in Figure 1. Test compounds caffeine, salicylic acid, and testosterone, were selected based on their historical prevalence in permeation studies performed both in vitro [24, 25] and in vivo [26–28], as well as their range of physicochemical properties known to influence dermal absorption, including lipophilicity, polarity, and solubility [29]. [8-^{14}C]-Caffeine (specific activity of 55 mCi/mmol, product # ARC 1377, lot # 210914), [7-^{14}C]-salicylic acid (specific activity of 55 mCi/mmol, product # ARC 0324, lot # 210914), and [4-^{14}C]-testosterone (specific activity of 55 mCi/mmol, product # ARC 0858, lot # 210902) formulated in ethanol were purchased from American Radiolabeled Chemicals Inc. (St. Louis, MO, USA). Stock solutions of radiolabeled caffeine and salicylic acid were diluted in 1X phosphate buffered saline (PBS; Corning Inc., Corning, NY, USA) to a working concentration for IVPT of 0.61 nmol/μL (0.33 μCi/10 μL). Radiolabeled testosterone was diluted to the same concentration in 100% ethanol (Decon Labs Inc., King of Prussia, PA, USA) for improved solubility. For vehicle effect experiments, additional working solutions of radiolabeled caffeine and salicylic acid were prepared with 100% ethanol, again to a working concentration of 0.61 nmol/μL. Working concentrations were verified by mixing 10 μL of sample with 20 mL of liquid scintillation cocktail (Ultima Gold; PerkinElmer, Waltham, MA, USA), and assessing ^{14}C disintegrations per minute with a Tri-Carb 4910TR liquid scintillation counter (PerkinElmer). The tissue solubilizer, SOLVABLE, was purchased from PerkinElmer.

3.2 Excised Human Skin and Alternative Skin Barrier Model Storage and Handling

EHS was purchased from BioIVT (Westbury, NY, USA). Human skin was collected from the abdominal region of three consenting female donors undergoing elective surgery, under an Institutional Review Board (IRB)-approved protocol. After collection, EHS was dermatomed to a thickness of 350 μm and stored at −60 °C until use. EpiDerm RhE (EpiDerm-200-X; part # EPI-200-X, 8 mm usable tissue diameter) was purchased from MatTek (Ashland, MA, USA) and stored at 4 °C upon arrival, following the manufacturer's recommendations. Strat-M synthetic dermal barrier membranes (diameter of 2.5 cm, catalog # SKBM02560) were purchased from Sigma-Aldrich (St. Louis, MO, USA) and stored at room temperature. Excised human skin donor information can be found in the supplemental material (Table S1).

3.3 In Vitro Permeation Testing Apparatus

Vertical Franz diffusion cells (PermeGear, Hellertown, PA, USA) with orifice diameters of 5 (product # 4G-01-00-05-05) or 15 mm (product # 4G-01-00-15-07) corresponding to application areas of 0.20 and 1.77 cm^2, respectively, were integrated into a Phoenix DB-6 dry heat diffusion system (Teledyne Hanson Research, Chatsworth, CA, USA). The Phoenix DB-6 was adapted with custom-made inserts to ensure good contact between the FCs and the DB-6 surface. The water jacket portions of the FCs were connected in series with silicone tubing and integrated with a CORIO CD-BC4 heated water circulator (JULABO GmbH, Seelbach, Germany). Both the dry heat system and heated water circulator were

set to 32.5 °C for the entirety of the experiment to ensure that a physiological human skin temperature (32 °C) was maintained.

3.4 Tissue and Membrane Mounting

EHS was transferred on dry ice to the IVPT setup and appropriately sized sections, dependent on FC selection, were cut while the tissues remained frozen. EHS was then transferred to the FC, epidermis side up, and gently stretched to ensure complete and wrinkle-free coverage of the orifice. The donor chamber portion of the FC was then placed on the apical skin surface and the two FC components and skin section were fixed together with the FC manufacturer's provided metal clamp.

For EpiDerm-200-X samples, transwells were sterile-transferred to 6-well plates with 0.9 mL warmed (37 °C) assay medium (MatTek, part # EPI-100-NMM-ASY) in each well. Tissues in media were transferred to an incubator (Heracell VIOS 160i; Thermo Fisher Scientific, Waltham, MA, USA) and kept at 37 °C with 5% CO_2 for a minimum of 1 h. Excess samples (when not all used on Day 1) were exposed in open packaging to a 5% CO_2 environment for 15 min, sealed, and transferred back to 4 °C overnight, as recommended by manufacturer. After incubation, EpiDerm-200-X transwells were removed from media and the tissue was cut from the insert with its support membrane using a scalpel, taking care not to damage the integrity of the tissue. The EpiDerm-200-X samples and support membrane were then mounted on the 5 mm diameter orifice FC, with the epidermal side facing up, making sure that they fully covered the diffusion area. Care was taken to avoid wrinkles or disruption of the tissue during donor chamber placement and clamping.

In addition to the biological skin barrier models, the synthetic membrane, Strat-M, was evaluated for IVPT. Strat-M is a lipid-functionalized, multi-layered porous membrane comprising a very tight top layer, followed by two layers of polyethersulfone, and a basal layer of polyolefin non-woven fabric support [30]. The layers of Strat-M increase in thickness and permeability from the apical to basal side of the membrane, analogous to the layers of human skin (epidermis, dermis, and hypodermis). For IVPT, Strat-M membranes were removed from their packaging and mounted directly on the FCs, shiny side up. Regardless of skin barrier model used, mounted FCs were filled with pre-sonicated, warmed (32 °C) 1X PBS to the specified volume (5 or 7 mL for 5 and 15 mm diameter orifice FCs, respectively), ensuring no bubbles were present. A magnetic stir bar was added to each receptor compartment and rotated at 400 rpm to maintain uniform temperature and solution over the course of the IVPT experiment.

The temperature of the mounted skin barrier models was monitored with a Fluke 62 max IR thermometer (Everett, WA, USA) until they reached a steady temperature of 32 °C.

3.5 Transepidermal Water Loss

Mounted and warmed skin barrier models (EHS, EpiDerm-200-X, and Strat-M) were analyzed by measuring their transepidermal water loss (TEWL) with a VapoMeter (Delfin Technologies Ltd, Kuopio, Finland). Depending on the orifice diameter of the FC used, a cell-specific adaptor was employed to ensure a good seal was achieved around the upper

portion of the donor chamber. EHS samples with a TEWL greater than 10 g/m^2 h were excluded from experimentation and analyses, as recommended [31].

3.6 Dosing and Sample Collection

A finite dose (10 μL/cm^2, 6 nmol/cm^2) of freshly prepared working solutions of radiolabeled chemicals was used for all experiments. The experimental dose was selected to achieve sufficient radioactivity for detection, as informed by previous work [25], as well as to normalize molar concentration across test chemicals. The topical dose was applied with a Pos-D positive displacement pipette (Mettler-Toledo Rainin, LLC, Oakland, CA, USA) directly to the center of the tissue or membrane. Receptor fluid samples (500 μL) were collected through the FC sample port at 0.5, 1, 2, 3, 4, and 6 h post-dosing with a 1 mL Hamilton glass syringe fitted with a 4", 16-gauge metal needle (Cadence Science Inc., Cranston, RI, USA), and transferred directly to glass scintillation vials (Thermo Fisher Scientific; "receptor" sample). Immediately following sample collection, the receptor solution volume was restored to its initial volume by adding 500 μL of fresh, warmed (32 °C) 1X PBS into the sample port, taking care not to introduce air bubbles. Dosing and sampling across FCs were performed in 45 s intervals to ensure consistent time points. At 6 h, the apical skin surface was washed by pipetting 100 μL (5 mm FC) or 500 μL (15 mm FC) 100% ethanol into the donor chamber and removing the ethanol and unbound compound with a cotton cosmetic pad. A second cotton pad was used to ensure all unbound compound was collected. The two cotton pads were transferred to a scintillation vial for analyses ("donor" sample). After washing, tissue or membrane samples were removed from their FC and transferred in their entirety to scintillation vials containing 2 mL of SOLVABLE. Tissue/ Membrane samples in SOLVABLE were then placed in an orbital incubator (Gyromax 737, Amerex Instruments, Inc., Concord, CA, USA) set to 150 rpm and 60 °C and digested overnight ("tissue" sample). All samples were mixed with 20 mL of Ultima Gold and transferred to the scintillation counter for radioactivity measuring. Intra- and inter-day variability of the outlined IVPT method was evaluated and found to be minimal (Figure S1).

3.7 Histology

Histology was performed as previously described [32]. Briefly, EpiDerm-200-X samples were washed with 1X PBS and fixed in 10% neutral buffered formalin for at least 24 h. After fixation, the samples with their support membrane were excised from the culture inserts with a scalpel. For EHS, frozen tissue samples (approximately 1 cm^2) were briefly thawed before transferring to embedding cassettes and submerging in 10% neutral buffered formalin for at least 7 days. All fixed samples were routinely processed, trimmed (bisected), and embedded in a paraffin-based infiltrating media (Formula 'R', Leica Biosystems, Wetzlar, Germany), sectioned at 4–6 μm, and mounted on glass microscope slides. Slides were stained with hematoxylin and eosin (H&E) using a Leica Autostainer and evaluated by light microscopy. Representative micrographs were captured using a Nikon Eclipse Ni-E Upright Motorized Microscope (Tokyo, Japan).

3.8 Data Analysis

Three primary IVPT metrics were calculated: cumulative amount permeated, flux, and mass distribution. Cumulative amount permeated at each time point was calculated as follows:

$$\text{When n = 1, } Cumulative \ Amount = \left(\frac{RF_n}{V_s}\right)V_R$$

$$\text{When n > 1, } Cumulative \ Amount = \left(\frac{RF_n}{V_s}\right)V_R + \left(\sum_{i=1}^{n-1} RF_i\right)$$

Where RF_n is the amount of permeant in receptor fluid sample n, V_s is the volume sampled (500 µL), and V_R is the total volume of the receptor compartment (5 or 7 mL). Sample n = 1, 2, 3, 4, 5, or 6 corresponds with samples taken at times 0.5, 1, 2, 3, 4, and 6 h after dose application, respectively. Resulting cumulative amounts were normalized to the application area of the FC used (reported as nmol/cm^2) and plotted over time.

Flux, reported as nmol/cm^2/h, was calculated by dividing the amount of chemical permeated between collections by the time between collections. The mass distribution was calculated by dividing the total amount of radiolabeled chemical found in either the receptor, tissue, or donor samples after the completion of the experiment by the amount of test chemical applied to the apical skin surface at dosing (reported as % of dose). The mass balance was calculated as the sum of the three compartments.

All IVPT experiments were performed in triplicate (three individual FCs) for each donor/batch and condition and three independent donors/batches were used, except where indicated. Data are reported as the mean ± standard error of mean (SEM). Statistical analyses were performed in Prism (GraphPad Software, Inc., San Diego, CA, USA) or SAS (SAS Institute, Cary, NC, USA).

Statistical analyses of IVPT metrics were conducted for comparison of FC (5 mm versus 15 mm), chemical (caffeine, salicylic acid, and testosterone), and vehicle (33% ethanol versus 100% ethanol). Values were averaged across replicated measurements. The cumulative amount was analyzed for each skin barrier model using a repeated measures analysis of variance (ANOVA) with pairwise comparisons of main effects adjusted using Tukey's test and subgroup effects adjusted using the maximum modulus test. The FC comparison included the main effects of FC and chemical, the chemical analysis included the main effect of chemical, and the vehicle analysis included the main effects of vehicle and chemical (caffeine and salicylic acid only). Mass distribution for each of the three comparisons was analyzed for each skin barrier model by one-way or two-way ANOVA of the arcsine-square root transformed recovery (proportion of dose), using the same main effects as for cumulative amount. Pairwise comparisons of main effects were performed using adjusted Tukey's test and subgroup effects were adjusted using the maximum modulus test.

Additionally, statistical analyses were conducted for comparison of skin barrier model (EHS, Strat-M, and EpiDerm-200-X). Values were averaged across replicated measurements.

Cumulative amount was analyzed using a two-way repeated measures ANOVA with pairwise comparisons of main effects adjusted using Tukey's test and subgroup effects adjusted using the maximum modulus test. Mass distribution was analyzed for each skin barrier model by two-way ANOVA of the arcsine-square root transformed recovery (proportion of dose), using the same main effects as for cumulative amount and flux. Pairwise comparisons of main effects were performed using adjusted Tukey's test and subgroup effects were adjusted using the maximum modulus test.

4   Results

4.1   Comparison of IVPT outcomes in different diameter orifice Franz cells

First, we sought to assess the influence of FC orifice size on IVPT outcomes. FCs with a standard orifice diameter of 15 mm were directly compared to those with a less common, but more skin barrier model-compatible, diameter of 5 mm. Permeation of a finite dose (6 nmol/cm^2; 10 μL/cm^2) of caffeine was quantified through both EHS and the synthetic skin barrier membrane, Strat-M, when mounted on either 5 mm or 15 mm diameter orifice FCs (Figure 2). The cumulative amount permeated (top row), flux (middle row), and the mass distribution of the dose applied (bottom row) were quantified.

The permeation of caffeine (Log K_{ow} = −0.07) through EHS was statistically indistinguishable across FC sizes, suggesting no influence of FC orifice diameter on permeation rate (Figure 2A). The respective results for Strat-M were similarly not significantly different; however, the peak flux was earlier in the 5 mm orifice FC compared to the 15 mm FC (1 and 2 h, respectively; Figure 2B). The permeation of salicylic acid (Log K_{ow} = 2.26; Figure S2) and testosterone (Log K_{ow} = 3.32; Figure S3) through EHS and Strat-M was additionally quantified when the skin barrier models where mounted on 5 mm or 15 mm orifice FCs. As with caffeine, similar permeations of salicylic acid and testosterone through EHS were observed across FC orifice sizes; however, they tended to be higher on 5 mm orifice FC compared to 15 mm, with variable statistical significances, in the Strat-M model. Together, these results highlight the importance of utilizing consistent FC sizes within studies if data are to be compared. Nonetheless, these data support that when utilizing alternative models of skin that are not suitable for larger orifice FCs, the use of a FC with an orifice as small as 5 mm in diameter is feasible. As such, FCs with an orifice diameter of 5 mm were used for the remainder of the study. Of note, the diameter of the tissue mounted on the FC was not found to influence IVPT outcomes (Figure S4).

4.2   Assessing histological and barrier variability amongst excised human skin donors and commercially available reconstructed human epidermis batches

A key consideration in the design of permeation experiments is the number of donors and number of replicate samples. EHS barriers have inherent variability due to donor sex, age, race/ethnicity, and anatomical site, amongst others; however, the degree to which independent batches of reconstructed skin barrier models, that is, samples that are grown on separate days, preferably with different cell pools, vary in their barrier remains poorly understood. Thus, we evaluated, in parallel, EHS from three different donors and three independently received batches of EpiDerm-200-X for morphology and barrier. Sections

of EHS were stained with H&E and examined under a brightfield microscope (Figure 3A). EHS sections appeared to have slight differences in the thickness and structure of the epidermis across donors. These inherent variabilities are reflected, in part, by the barrier analysis with TEWL, as excised skin from the first donor had a significantly higher mean TEWL, compared to the third donor (Figure 3B). Interestingly, while histological analysis of EpiDerm-200-X showed minimal changes in overall tissue thickness or structure across batches (Figure 3C), the second batch received had significantly higher mean TEWL compared to the first and third batch (Figure 3D). Despite the statistical significances observed, the absolute differences in mean TEWL across donors or batches were relatively minimal (within 3 g/m^2 h of each other). How the amount of change in TEWL reflects a change in the barrier to compound permeation remains to be determined. Nonetheless, these results highlight both the inherent variability of human donor skin barriers, as well as the potential for barrier variability when reconstructed epidermis is grown in independent batches. Of note, the mean TEWL for all batches of EpiDerm-200-X was ~6-fold higher than that of EHS. EHS from three donors or three independent batches of EpiDerm-200-X were used for all remaining experiments.

4.3 Ranking permeation of reference compounds through excised human skin, Strat-M, and EpiDerm-200-X

The benefits of skin barrier models in permeation studies may be to, 1) predict the rate and amount of compound dermally absorbed over a relevant time interval, or 2) understand how a specific compound's permeation metrics rank within a known set of chemicals. While the former would be the ultimate goal in pursuit of a physiological skin barrier model, the latter may be informative as a qualitative predictor of dermal penetration. In this study, we quantified the permeation of select compounds over 6 h, and considered both the amount each permeated across skin barrier models and how the compound's ability to permeate the skin barrier ranks within each model. The permeation of a finite dose (6 $nmol/cm^2$; 10 $\mu L/cm^2$) of caffeine, salicylic acid, and testosterone, three compounds used in cosmetic or topical drug products that span a range of physicochemical properties known to influence skin permeation, was quantified. Permeation experiments were performed on EHS, EpiDerm-200-X, or Strat-M mounted on 5 mm orifice FCs. Of the compounds tested, caffeine showed a higher mean permeation (0.97 ± 0.22 $nmol/cm^2$) over 6 h in EHS than testosterone (0.33 ± 0.13 $nmol/cm^2$) and salicylic acid (0.18 ± 0.10 $nmol/cm^2$) (Figure 4A).

The synthetic skin barrier membrane, Strat-M, restricted the permeation of testosterone (6 h cumulative permeation of 0.05 ± 0.03 $nmol/cm^2$), but was relatively permissive to the permeation of both caffeine (0.43 ± 0.03 $nmol/cm^2$) and salicylic acid (0.68 ± 0.13 $nmol/cm^2$) (Figure 4B). Interestingly, the flux profile of caffeine through Strat-M (i.e., the rate of compound permeation between each collection time) showed an early peak in permeation rate, around 1 h, that rapidly fell and stabilized over the remainder of the experiment, whereas the flux of salicylic acid through Strat-M steadily increased over the first 3 h prior to stabilizing.

In EpiDerm-200-X, caffeine and testosterone showed similar levels of permeation (3.32 ± 0.33 and 2.99 ± 0.31 $nmol/cm^2$, respectively) at 6 h post-dosing, with both amounts

being significantly higher than that of salicylic acid (0.32 ± 0.05 nmol/cm^2; Figure 4C). Considering the flux profiles, testosterone had a slightly earlier mean peak flux compared to caffeine (2 h versus 3 h, respectively), despite comparable cumulative permeation at 6 h. This is similar to the flux patterns of testosterone and caffeine through EHS, although at a different scale.

In addition to quantifying the total amount of compound that was able to completely permeate the skin barrier model ('Receptor'), the amount of compound remaining unbound on the apical surface of the skin barrier model ('Donor') and the amount of compound absorbed into the tissue but not released to the receptor fluid ('Tissue') were determined (Figure 4, bottom row). Except for testosterone in EHS, in which most compound remained in the donor compartment, the majority of the compound that was not found in the receptor fluid was retained in the tissue at 6 h post-dosing. Overall, the proportion of compound that remained unbound on the apical surface of the skin barrier models was lowest in EpiDerm-200-X.

When considering just the ranking of the mean 6 h cumulative amount of compound in the receptor fluid, caffeine permeated the most, followed by testosterone, and finally salicylic acid in EHS and EpiDerm-200-X. In Strat-M, salicylic acid showed the highest level of permeation, followed by caffeine and finally testosterone. Importantly, however, the fold differences in these amounts and the statistical significances varied greatly. A summary of these comparisons, as well as the statistical comparison of each compound's mean 6 h cumulative permeation across skin barrier models, can be found in Table 1.

4.4   Evaluating vehicle influence on permeation with alternative skin barrier models

Another area addressable by skin barrier models is in evaluating an effect of vehicle formulation on dermal absorption. For example, cosmetics and topical drugs alike are delivered in a vehicle, often tailored to permit compound solubility and facilitate consumer application. Understanding how vehicles influence the permeation of a compound of interest is critical in the safety assessment of such products. Here, we sought to evaluate the permeation of caffeine and salicylic acid when delivered in two different vehicles. EHS, Strat-M, and EpiDerm-200-X were mounted on 5 mm orifice FCs. Stock radiolabeled caffeine diluted in either PBS (final formulation of 33% ethanol) or ethanol (final formulation of 100% ethanol) was applied to the apical tissue surface (6 nmol/cm^2; 10 μL/cm^2) and their permeation was quantified. A statistically significant decrease in 6 h caffeine cumulative permeation was observed through Strat-M and EpiDerm-200-X, but not EHS, when delivered in 100% ethanol versus 33% ethanol (Figure 5A–C). Similar results were observed with EHS and Strat-M when salicylic acid was delivered in the two vehicles (Figure 6A–B). As for EpiDerm-200-X, however, the delivery of salicylic acid in the higher percentage ethanolic vehicle did not alter its permeation (Figure 6C), similar to the results observed in EHS (Figure 6A).

5   Discussion

Despite decades of research into the design and development of reconstructed skin and skin barrier models, more data are needed to increase confidence in the ability of such

models to mimic the physiological human skin barrier, including in the context of IVPT. Here, two alternative skin barrier models were selected for comparison to EHS, Strat-M and EpiDerm-200-X. These two models represent two major classes of alternative skin barrier models, synthetic barrier membranes (Strat-M) and RhE (EpiDerm-200-X). While other RhE models exist, the EpiDerm™ line was the primary focus of our study given the prevalence of its use in literature to date [19, 33, 34]. EpiDerm-200-X was selected over other variations of the EpiDerm line due to the manufacturer's recommendations for percutaneous absorption studies (www.mattek.com) and the desire to minimize tissue use and maximize throughput. Limitations and benefits exist for the tissues and tissue models used in this work with relation to storage and handling prior to IVPT. Strat-M membranes, for example, are relatively affordable and are delivered and stored at room temperature, and thus do not require extra equipment. EHS, in contrast, requires an ultra-low temperature freezer for storage if barrier properties are to be preserved. This, in addition to the cost and logistics of obtaining the tissue, can hinder the conduct of large scale IVPT studies. Overall handling and use of EHS, however, is relatively straightforward and requires minimal training. EpiDerm-200-X is the most involved model utilized here, in terms of handling, storage, and preparation. As a live cell culture, EpiDerm-200-X requires all the necessary cell culture equipment, including a biological safety cabinet for sterile transfer of tissues to media and a cell culture incubator. While all this equipment stated may be routinely used in laboratories currently interested in utilizing alternative skin barrier models, it is well documented that the cost of technical resources is a major barrier towards adoption of alternative models (e.g., microphysiological systems) for regulatory research [35]. Awareness of how these technical and financial aspects affect the potential success of skin barrier models for in vitro percutaneous absorption studies is critical moving forward. Ideally, this should be balanced with the overall benefit and reliability of the model of interest.

IVPT can be performed in a variety of diffusion cell systems. One commonly used diffusion cell model is the static Franz diffusion cell [14]. The application area of a traditional FC can be described as the surface area of the tissue exposed to the basal receptor media and apical air, where the test compound is applied. FCs with an array of application areas, defined by the diameter of the orifice, are available, and the use of a certain size is not universal in literature. Typically, studies of percutaneous absorption aim to describe the permeation behavior of the compound of interest by measuring the cumulative amount of compound permeated over time. This outcome can be described by Fick's first law of diffusion, which states that the rate of diffusion of a substance across a unit area is proportional to the concentration gradient [36]. Given that the diffusion coefficient and concentration gradient, under sink conditions, are independent of the application area, Fick's law suggests that the flux should therefore be consistent across different FC orifice diameters when the dose is applied at a consistent and uniform concentration per unit area of the orifice [36]. Previously, Dreher and colleagues [34] quantified the permeation of benzoic acid and caffeine through the commercially available RhE, EpiSkin, when mounted on flow-through diffusion cells with application areas ranging from 0.28 to 0.5 cm^2. Compounds were applied both in a specified volume and concentration per unit of the application area. While

some variability was observed, no significant differences in the permeation profiles were detected across application areas tested, as expected based on Fick's first law.

Here, we investigated the influence of static Franz diffusion cell orifice diameter on the permeation metrics of caffeine, as well as salicylic acid and testosterone. One difference between this work and the work of Dreher et al. is that we applied a finite dose (10 μL/cm^2) versus their infinite dose (125 μL/cm^2). This difference is important in interpreting the results across studies, as while the flux as defined by Fick's first law should not be influenced by this change, the law assumes uniform application of the dose over the surface of the tissue. With an infinite dose, the volume of the formulation applied is sufficient to cover the membrane surface, while a finite dose requires spreading. Finite dosing, however, more closely mimics the clinical/"real world" application of dermatological products [36], hence its use herein. For all compounds tested, we observed that cumulative permeation across EHS was similar regardless of whether a 5 mm or 15 mm diameter orifice FC was used. Interestingly, more variability was observed when measuring permeation of the compounds across the synthetic membrane, Strat-M. We hypothesize that this difference may be due to Strat-M being dry during application, which translates to more difficulty in spreading the liquid dose, and thus may result in greater experimental variability. While the EHS apical surface is not moistened prior to experimentation, the biological nature of the EHS may be that it is more prone to retain the applied dose over a consistent unit of area, explaining the decreased experimental variability observed. Of note, the spreading of the dose may also be more challenging in the smaller orifice FC given the confined nature of the donor chamber. Together, the data presented urge caution when comparing results obtained with different size diffusion cell application areas or under varying dose conditions. Nevertheless, absolute differences were relatively minimal and a well-controlled and consistent study should be unaffected by application area. The ability to utilize diffusion cells with smaller application areas can increase the flexibility when selecting a tissue barrier model for IVPT, and thus should be pursued.

Three compounds covering a range of skin permeation-relevant physicochemical properties and found in cosmetics or topical drugs were selected for permeation testing herein: caffeine, testosterone, and salicylic acid. Caffeine and testosterone are additionally recommended in the OECD Test Guideline No. 428 for use as IVPT reference chemicals. We found that the dermal absorption of salicylic acid through EpiDerm-200-X was similar to that of EHS, while the permeation of testosterone and caffeine was substantially increased through EpiDerm-200-X. Previously, Schmook and colleagues [24] quantified the dermal absorption and flux of a range of dermatological drugs through EHS and the commercially available RhE, SkinEthic™, mounted on Franz diffusion cells. SkinEthic was a poor barrier to the more hydrophobic drugs (hydrocortisone, clotrimazole, and terbinafine) when compared to EHS. In contrast, SkinEthic mostly retained salicylic acid in the tissue, which was similar to what was observed in EHS. These results are in alignment with those reported herein, as the RhE tested, EpiDerm-200-X, limited the permeation of salicylic acid, but was comparatively permissive to the permeation of the hydrophobic compound, testosterone.

The discrepancy between permeation of hydrophilic versus hydrophobic compounds through EHS and the RhE model reported herein and elsewhere may be due in part to the differential

modes of passage and lipid content of the *stratum corneum*. While low-molecular-weight hydrophobic compounds, such as testosterone, permeate by free volume diffusion through the lipid bilayers, hydrophilic compounds, such as caffeine, pass through pores in the *stratum corneum* without interacting with lipid bilayers [37]. Therefore, it could be hypothesized that the pore characteristics of the *stratum corneum* of RhE are like those of human skin, making such models similar in their barrier properties towards the permeation of hydrophilic molecules. In contrast, difficulties in replicating the lipid content and structure of the *stratum corneum* in RhE may limit their potential to mimic the human skin barrier to hydrophobic molecules. In a study by Tfayli and colleagues [38], the researchers utilized high-performance liquid chromatography (HPLC) and Raman spectroscopy to examine the lipid profile of the *stratum corneum* of EHS and EpiDerm RhE. HPLC analysis revealed that the *stratum corneum* of the RhE had all lipids found in the EHS samples; however, the relative amounts differed significantly. Additionally, Raman spectrographs depicted lipids primarily in droplets or separate zones, highlighting the discontinuity of the lipid barrier of the RhE. These data support the hypothesis that RhE models fail to replicate the intricate lipid structure of human skin *stratum corneum*, and thus are limited in their ability to replicate the human skin barrier to compounds affected by such parameters. Future work optimizing alternative skin barrier model development to replicate these critical lipid characteristics of the human *stratum corneum* will be beneficial going forward.

As for the permeation of hydrophilic drugs, the results may be influenced by additional factors. Previous work by Schreiber et al. [19] examined the permeation of caffeine and testosterone through heat separated human epidermis and two RhE models, EpiDerm and SkinEthic, mounted on FCs. Similar to the results observed herein, both caffeine and testosterone permeation was significantly higher in the RhE models compared to the human epidermal sheets. The increase in permeation of caffeine in the RhE, despite being a hydrophilic molecule, may be due to the polar nature of the compound. Polar molecules like caffeine are known to bind the polar heads of lipids, and thus are influenced by the uniformity of the *stratum corneum* [39]. Given that salicylic acid is less polar compared to caffeine, the differences in the permeation results observed (caffeine increased in RhE, while salicylic acid did not) may be explained by these interactions. Further expanding the pool of test chemicals in future IVPT experiments may help clarify these findings.

Besides replicating the *stratum corneum* with biological models, synthetic membranes that mimic characteristics of this key component of the skin barrier have shown promise in basic mechanistic studies [40]. The synthetic skin barrier model evaluated here, Strat-M, limited the passage of testosterone to a degree similar to that of EHS. The passage of both caffeine and salicylic acid, however, was significantly different in Strat-M versus that in EHS. Additionally, the overall rank of the cumulative permeation in Strat-M of the three compounds tested failed to match that of EHS. These results are in partial alignment with those of Uchida et al. [21], in which the correlation between permeation of an array of molecules through EHS and Strat-M neared 1, but varied depending on the compound tested. Additional data provided by our work, importantly, is the mass distribution of the compounds through the system at the end of the experiment. The ability of a compound to permeate into and integrate with the epidermis, sometimes described as the partition coefficient in the skin, is important when defining its dermal delivery [41],

and is better interpreted when mass distribution data are provided. Overall, the permeation results presented are highly variable depending on the alternative skin barrier model tested, stressing the importance of defining 'fit-for-need' applications of specific models until an 'ideal' model of the human skin barrier is developed.

Cosmetic and topical drug products are formulated in vehicles to aid in the delivery of the active compounds to the skin layer of interest. These vehicles can include an array of solid and semi-solid formulations (e.g., creams, gels), as well as liquid formulations (e.g., oils) depending on the use. In addition to mediating dermal absorption, vehicle formulation may also influence the spreading of the compound over the application area of the tissue under finite dose condition. Hence, it is important that any alternative skin barrier model used for IVPT be able to discern these vehicle effects. Here, we compared the permeation of caffeine and salicylic acid across EHS and alternative skin barrier models when delivered in either 33% ethanol or 100% ethanol. In all cases, delivering the compounds in 100% ethanol resulted in a net reduction in permeation; however, the degree of the reduction and statistical significances differed, with 100% ethanol altering the permeation of both caffeine and salicylic acid through Strat-M the most and EHS the least. These results are in part reflective of those found in work by Hewitt and colleagues [25], where a decrease in permeation of select compounds through EHS was observed when delivered in 100% ethanol versus PBS. The authors hypothesized that the decrease in permeation observed may have been due to a higher rate of evaporation of the 100% ethanol vehicle when compared to PBS, resulting in greater compound precipitation and thus restricting its ability to permeate the skin barrier. Of note, in Strat-M in the work presented herein, where the largest decrease in permeation was observed, the total compound mass collected at the end of the experiment when 100% ethanol vehicle was employed was generally reduced (ranging from 82–85% of dose) compared to the 33% ethanol vehicle (ranging from 92–96% of dose). Thus, it cannot be ruled out that the decreased permeation observed with Strat-M is in part a result of difficulty in sample collection and analysis. Future work should explore further vehicle formulations and how they alter permeation of relevant chemicals in alternative skin barrier models.

To conclude, alternative skin barrier models require continued improvement if they are to directly replicate the intricate human skin barrier and be used as a tool to predict permeation of chemicals across the human skin. Establishing a comprehensive experimental flow to evaluate existing and novel alternative skin barrier models in direct comparison to EHS is critical to progress the field. We propose first selecting an FC with a suitable orifice diameter to use consistently throughout the evaluation. Next, a range of compounds spanning physicochemical properties relevant to skin permeation should be tested. While only three compounds were tested here, over a 6 h permeation window, increasing the number of compounds tested and the length of exposure is likely to increase the impact of the assessment. Given the inherent variability of donor skin, excised skin from multiple donors should be tested. While it is assumed that reconstructed skin models are less variable than human skin, we suggest multiple batches be used, preferably constructed with independent cell pools on separate days. Finally, the alternative skin barrier model should be capable of detecting vehicle-dependent changes in compound permeation and should be evaluated for such. Utilizing the experimental and analytical framework provided herein

has the potential to address these questions, paving the way towards identifying promising alternative skin barrier models for in vitro dermal absorption studies.

Supplementary Material

Refer to Web version on PubMed Central for supplementary material.

Acknowledgments

8 Funding

11 Data Availability Statement

The datasets generated for this study can be found in part in the supplementary materials or from the corresponding author upon request.

12 References

1. Kolarsick PAJ, Kolarsick MA, and Goodwin C, Anatomy and physiology of the skin. Journal of the Dermatology Nurses' Association, 2011. 3(4): p. 203–213.

2. Abdo JM, Sopko NA, and Milner SM, The applied anatomy of human skin: a model for regeneration. Wound Medicine, 2020. 28: p. 100179.

3. Gilaberte Y, Prieto-Torres L, Pastushenko I, and Juarranz Á, Anatomy and function of the skin, in Nanoscience in Dermatology, Hamblin MR, Avci P, and Prow TW, Editors. 2016, Academic Press: Boston. p. 1–14.

4. DeLuca M, Tamura RN, Kajiji S, Bondanza S, Rossino P, Cancedda R, Marchisio PC, and Quaranta V, Polarized integrin mediates human keratinocyte adhesion to basal lamina. Proceedings of the National Academy of Sciences, 1990. 87(17): p. 6888–6892.

5. Bouwstra JA and Ponec M, The skin barrier in healthy and diseased state. Biochimica et Biophysica Acta, 2006. 1758(12): p. 2080–2095. [PubMed: 16945325]

6. Matsui T and Amagai M, Dissecting the formation, structure and barrier function of the stratum corneum. International Immunology, 2015. 27(6): p. 269–280. [PubMed: 25813515]

7. van Smeden J and Bouwstra JA, Stratum corneum lipids: their role for the skin barrier function in healthy subjects and atopic dermatitis patients. Curr Probl Dermatol, 2016. 49: p. 8–26. [PubMed: 26844894]

8. Chang RK, Raw A, Lionberger R, and Yu L, Generic development of topical dermatologic products: formulation development, process development, and testing of topical dermatologic products. American Association of Pharmaceutical Scientists Journal, 2013. 15(1): p. 41–52. [PubMed: 23054971]

9. Raney SG, Franz TJ, Lehman PA, Lionberger R, and Chen M-L, Pharmacokinetics-based approaches for bioequivalence evaluation of topical dermatological drug products. Clinical Pharmacokinetics, 2015. 54(11): p. 1095–1106. [PubMed: 26063051]

10. European Food Safety Authority (EFSA), Buist H, Craig P, Dewhurst I, Hougaard Bennekou S, Kneuer C, Machera K, Pieper C, Court Marques D, Guillot G, Ruffo F, and Chiusolo A, Guidance on dermal absorption. European Food Safety Authority Journal, 2017. 15(6): p. 4873.

11. Polak S, Ghobadi C, Mishra H, Ahamadi M, Patel N, Jamei M, and Rostami-Hodjegan A, Prediction of concentration–time profile and its inter-individual variability following the dermal drug absorption. Journal of Pharmaceutical Sciences, 2012. 101(7): p. 2584–2595. [PubMed: 22517028]

12. Settivari RS, Ball N, Murphy L, Rasoulpour R, Boverhof DR, and Carney EW, Predicting the future: opportunities and challenges for the chemical industry to apply 21st-century toxicity testing. Journal of the American Association for Laboratory Animal Science, 2015. 54(2): p. 214–223. [PubMed: 25836969]

13. Santos LL, Swofford NJ, and Santiago BG, In vitro permeation test (IVPT) for pharmacokinetic assessment of topical dermatological formulations. Curr Protoc Pharmacol, 2020. 91(1): p. e79. [PubMed: 32991075]

14. Franz TJ, Percutaneous absorption on the relevance of in vitro data. J Invest Dermatol, 1975. 64(3): p. 190–195. [PubMed: 123263]

15. Friend DR, In vitro skin permeation techniques. Journal of Controlled Release, 1992. 18(3): p. 235–248.

16. Schäfer-Korting M, Bock U, Gamer A, Haberland A, Haltner-Ukomadu E, Kaca M, Kamp H, Kietzmann M, Korting HC, Krächter HU, Lehr C-M, Liebsch M, Mehling A, Netzlaff F, Niedorf F, Rübbelke MK, Schäfer U, Schmidt E, Schreiber S, Schröder K-R, Spielmann H, and Vuia A, Reconstructed human epidermis for skin absorption testing: results of the German prevalidation study. Altern Lab Anim, 2006. 34(3): p. 283–294. [PubMed: 16831060]

17. Lehman PA, Raney SG, and Franz TJ, Percutaneous absorption in man: in vitro-in vivo correlation. Skin Pharmacol Physiol, 2011. 24(4): p. 224–230. [PubMed: 21455015]

18. World Health Organization, Dermal absorption. 2006, World Health Organization: Geneva.

19. Schreiber S, Mahmoud A, Vuia A, Rübbelke MK, Schmidt E, Schaller M, Kandárová H, Haberland A, Schäfer UF, Bock U, Korting HC, Liebsch M, and Schäfer-Korting M, Reconstructed epidermis versus human and animal skin in skin absorption studies. Toxicol In Vitro, 2005. 19(6): p. 813–822. [PubMed: 15913948]

20. Sinkó B, Garrigues TM, Balogh GT, Nagy ZK, Tsinman O, Avdeef A, and Takács-Novák K, Skin-PAMPA: a new method for fast prediction of skin penetration. Eur J Pharm Sci, 2012. 45(5): p. 698–707. [PubMed: 22326705]

21. Uchida T, Kadhum WR, Kanai S, Todo H, Oshizaka T, and Sugibayashi K, Prediction of skin permeation by chemical compounds using the artificial membrane, Strat-M™. European Journal of Pharmaceutical Sciences, 2015. 67: p. 113–118. [PubMed: 25447745]

22. Derr K, Zou J, Luo K, Song MJ, Sittampalam GS, Zhou C, Michael S, Ferrer M, and Derr P, Fully three-dimensional bioprinted skin equivalent constructs with validated morphology and barrier function. Tissue Eng Part C Methods, 2019. 25(6): p. 334–343. [PubMed: 31007132]

23. Zoio P, Lopes-Ventura S, and Oliva A, Biomimetic full-thickness skin-on-a-chip based on a fibroblast-derived matrix. Micro, 2022. 2(1): p. 191–211.

24. Schmook FP, Meingassner JG, and Billich A, Comparison of human skin or epidermis models with human and animal skin in in-vitro percutaneous absorption. Int J Pharm, 2001. 215(1–2): p. 51–56. [PubMed: 11250091]

25. Hewitt NJ, Grégoire S, Cubberley R, Duplan H, Eilstein J, Ellison C, Lester C, Fabian E, Fernandez J, Génies C, Jacques-Jamin C, Klaric M, Rothe H, Sorrell I, Lange D, and Schepky A, Measurement of the penetration of 56 cosmetic relevant chemicals into and through human skin using a standardized protocol. J Appl Toxicol, 2020. 40(3): p. 403–415. [PubMed: 31867769]

26. Bartek MJ, LaBudde JA, and Maibach HI, Skin permeability in vivo: comparison in rat, rabbit, pig and man. J Invest Dermatol, 1972. 58(3): p. 114–123. [PubMed: 4622425]

27. Taylor JR and Halprin KM, Percutaneous Absorption of Salicylic Acid. Archives of Dermatology, 1975. 111(6): p. 740–743. [PubMed: 1094962]

28. Wester RC and Maibach HI, Relationship of topical dose and percutaneous absorption in rhesus monkey and man. J Invest Dermatol, 1976. 67(4): p. 518–520. [PubMed: 823268]

29. Farahmand S and Maibach HI, Estimating skin permeability from physicochemical characteristics of drugs: A comparison between conventional models and an in vivo-based approach. International Journal of Pharmaceutics, 2009. 375(1): p. 41–47. [PubMed: 19481689]

30. Haq A, Goodyear B, Ameen D, Joshi V, and Michniak-Kohn B, Strat-M® synthetic membrane: permeability comparison to human cadaver skin. International Journal of Pharmaceutics, 2018. 547(1): p. 432–437. [PubMed: 29890259]

31. Zhang Q, Murawsky M, LaCount T, Kasting GB, and Li SK, Transepidermal water loss and skin conductance as barrier integrity tests. Toxicol In Vitro, 2018. 51: p. 129–135. [PubMed: 29698667]

32. Cao X, Lin H, Muskhelishvili L, Latendresse J, Richter P, and Heflich RH, Tight junction disruption by cadmium in an in vitro human airway tissue model. Respiratory Research, 2015. 16(1): p. 30. [PubMed: 25851441]

33. Schäfer-Korting M, Bock U, Diembeck W, Düsing H-J, Gamer A, Haltner-Ukomadu E, Hoffmann C, Kaca M, Kamp H, Kersen S, Kietzmann M, Korting HC, Krächter H-U, Lehr C-M, Liebsch M, Mehling A, Müller-Goymann C, Netzlaff F, Niedorf F, Rübbelke MK, Schäfer U, Schmidt E, Schreiber S, Spielmann H, Vuia A, and Weimer M, The use of reconstructed human epidermis for skin absorption testing: results of the validation study. Altern Lab Anim, 2008. 36(2): p. 161–187. [PubMed: 18522484]

34. Dreher F, Patouillet C, Fouchard F, Zanini M, Messager A, Roguet R, Cottin M, Leclaire J, and Benech-Kieffer F, Improvement of the experimental setup to assess cutaneous bioavailability on human skin models: dynamic protocol. Skin Pharmacol. Appl. Skin Physiol (Suppl 1), 2002. 15: p. 31–39. [PubMed: 12476007]

35. Rusyn I, Sakolish C, Kato Y, Stephan C, Vergara L, Hewitt P, Bhaskaran V, Davis M, Hardwick RN, Ferguson SS, Stanko JP, Bajaj P, Adkins K, Sipes NS, Hunter ES 3rd, Baltazar MT, Carmichael PL, Sadh K, and Becker RA, Microphysiological systems evaluation: experience of TEX-VAL tissue chip testing consortium. Toxicological Sciences, 2022. 188(2): p. 143–152. [PubMed: 35689632]

36. Lau WM and Ng KW, Finite and infinite dosing, in Percutaneous Penetration Enhancers Drug Penetration Into/Through the Skin: Methodology and General Considerations, Dragicevic N and Maibach HI, Editors. 2017, Springer-Berlin Heidelberg: Berlin. p. 35–44.

37. Mitragotri S, Modeling skin permeability to hydrophilic and hydrophobic solutes based on four permeation pathways. J Control Release, 2003. 86(1): p. 69–92. [PubMed: 12490374]

38. Tfayli A, Bonnier F, Farhane Z, Libong D, Byrne HJ, and Baillet-Guffroy A, Comparison of structure and organization of cutaneous lipids in a reconstructed skin model and human skin: spectroscopic imaging and chromatographic profiling. Experimental Dermatology, 2014. 23(6): p. 441–443. [PubMed: 24758415]

39. Roberts MS, Targeted drug delivery to the skin and deeper tissues: role of physiology, solute structure and disease. Clinical and Experimental Pharmacology and Physiology, 1997. 24(11): p. 874–879. [PubMed: 9363373]

40. Abd E, Yousef SA, Pastore MN, Telaprolu K, Mohammed YH, Namjoshi S, Grice JE, and Roberts MS, Skin models for the testing of transdermal drugs. Clin Pharmacol, 2016. 8: p. 163–176. [PubMed: 27799831]

41. Ellison CA, Tankersley KO, Obringer CM, Carr GJ, Manwaring J, Rothe H, Duplan H, Géniès C, Grégoire S, Hewitt NJ, Jamin CJ, Klaric M, Lange D, Rolaki A, and Schepky A, Partition coefficient and diffusion coefficient determinations of 50 compounds in human intact skin, isolated skin layers and isolated stratum corneum lipids. Toxicol In Vitro, 2020. 69: p. 104990. [PubMed: 32882340]
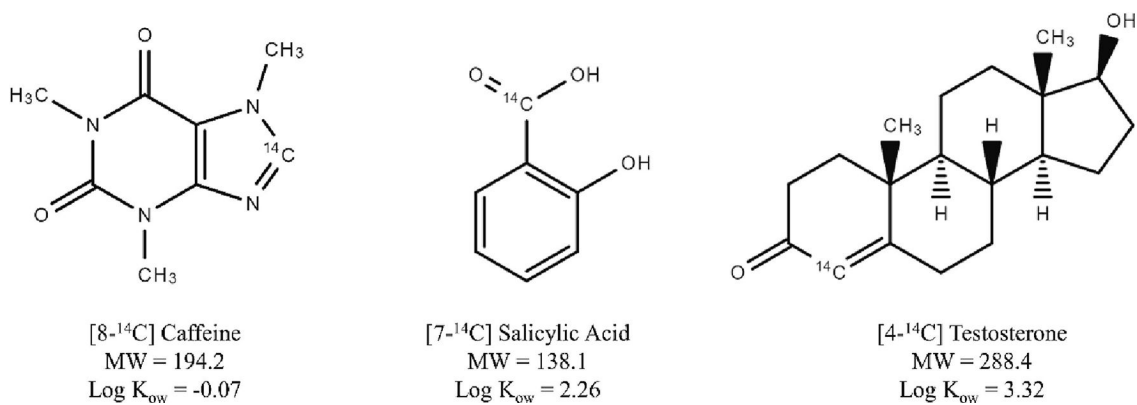
[8-^{14}C] Caffeine
MW = 194.2
Log K$_{ow}$ = -0.07

[7-^{14}C] Salicylic Acid
MW = 138.1
Log K$_{ow}$ = 2.26

[4-^{14}C] Testosterone
MW = 288.4
Log K$_{ow}$ = 3.32

Figure 1.
Chemical structures, molecular weights (MW, g/mol), and *n*-octanol-water partition coefficients (Log K$_{ow}$) of radiolabeled caffeine (CAS 58-08-2), salicylic acid (CAS 69-72-7), and testosterone (CAS 58-22-0) as used for in vitro skin permeation experiments.
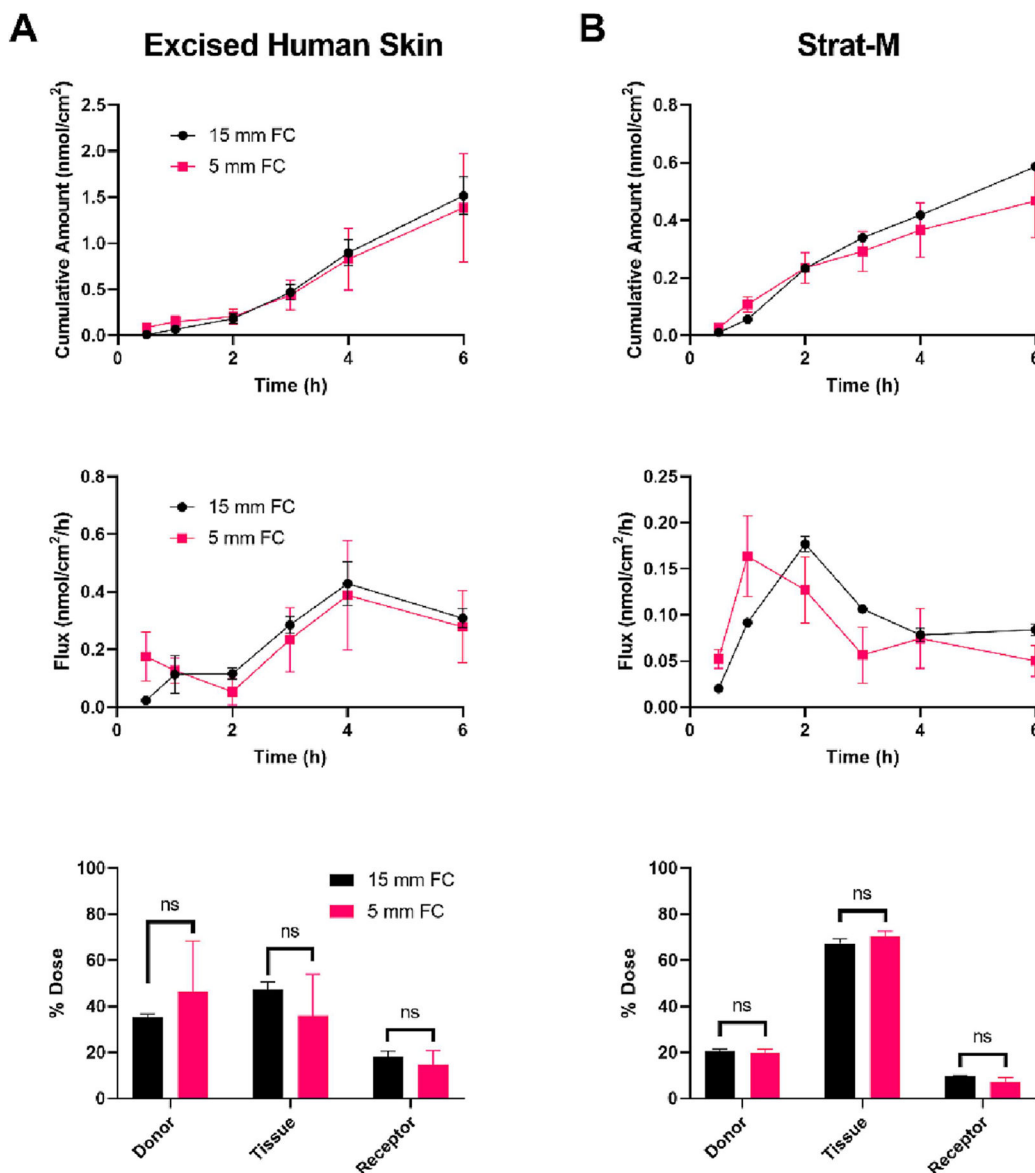
Figure 2.
Permeation of caffeine (Log K_{ow} = −0.07) through excised human skin (EHS) (A) and Strat-M (B) mounted on either 15 mm (black, circles) or 5 mm (red, squares) orifice Franz cells (FCs). A finite dose (6 nmol/cm^2; 10 μL/cm^2) was applied topically, and the cumulative amount permeated (top row), flux (middle row), and mass distribution (bottom row) were determined over 6 h. Mean cumulative amount across FC orifice sizes was statistically compared at each time point, for each model, by ANOVA with the maximum modulus test. Experiments performed in triplicate. Data shown as mean ± standard error of mean. No significant differences were observed. Mass distribution values were adjusted using an arcsin-square root transformation and the effect of FC orifice size within collection groups (i.e., donor, tissue, or receptor) was determined by ANOVA with the maximum modulus test. ns = no significance.
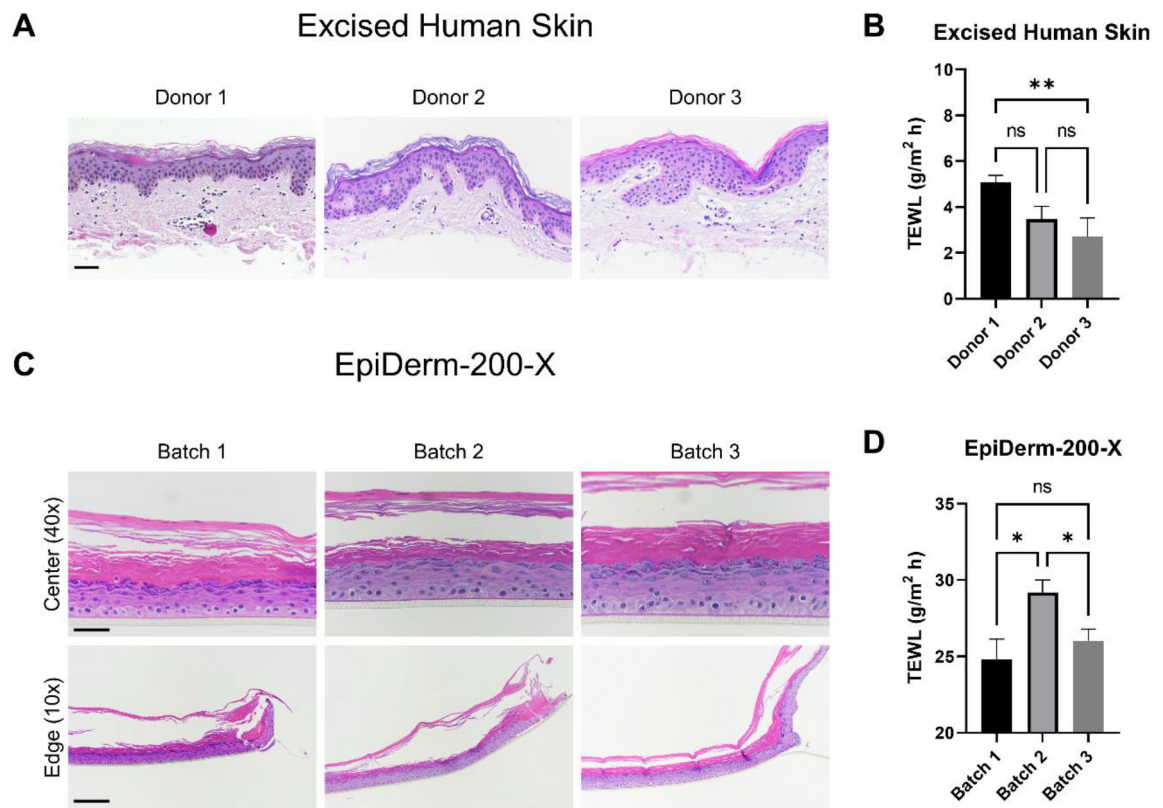
Figure 3.

Assessment of excised human skin (EHS) and EpiDerm-200-X reconstructed human epidermis morphological and barrier variability amongst donors/batches. EHS samples from three donors were fixed and processed for histological examination (A). Samples were stained with hematoxylin and eosin (H&E). Representative images are presented. Scale bar = 50 μm. Transepidermal water loss (TEWL) was measured on EHS samples mounted on 5 mm FCs (B). N = 6 – 20 samples per donor. The difference in mean TEWL was statistically compared by ANOVA with Tukey's test; ns = no significance, ** = p < 0.01. Three independently received EpiDerm-200-X batches were examined by histology (H&E; C) and TEWL (D) in an identical manner as EHS. Representative H&E images are presented. 40X scale bar = 50 μm; 10X scale bar = 200 μm. 'Center' and 'Edge' denote the portion of the tissue closest to the center or the edge of the transwell support upon which it was manufactured, respectively. N = 8 – 22 samples per batch. Data shown as mean ± standard error of mean. The difference in mean TEWL was statistically compared by ANOVA with Tukey's test; ns = no significance, * = p < 0.05.
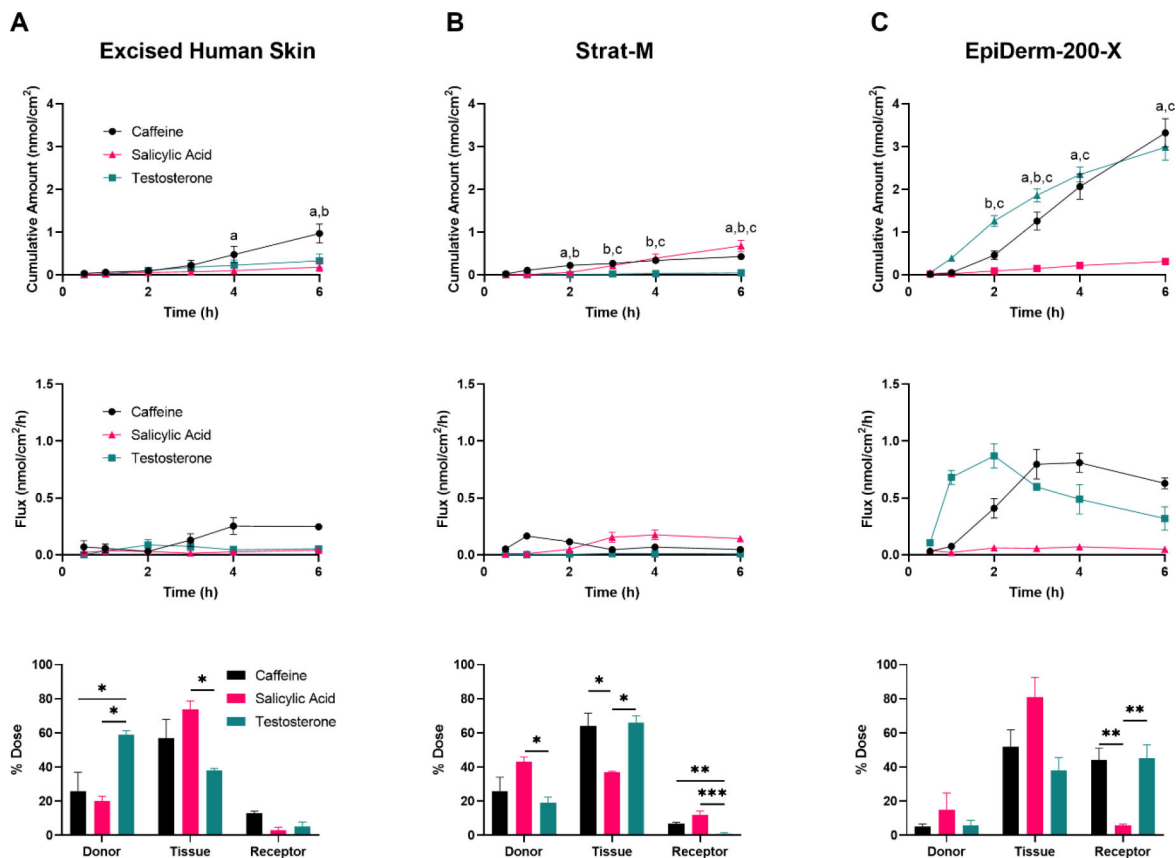
Figure 4.

Permeation of caffeine (Log K_{ow} = −0.07), salicylic acid (Log K_{ow} = 2.26), and testosterone (Log K_{ow} = 3.32) through excised human skin (EHS) (A), Strat-M (B), and EpiDerm-200-X (C). EHS and alternative skin barrier models were mounted on 5 mm orifice Franz cells and a finite dose (6 nmol/cm^2; 10 μL/cm^2) of the caffeine (black, circles), salicylic acid (red, triangles), or testosterone (green, squares) was applied topically. Cumulative amount permeated (top row), flux (middle row), and mass distribution (bottom row) were determined over 6 h. N = 3 donors/batches per barrier for each chemical, each in triplicate. Data shown as mean ± standard error of mean. Mean cumulative amount across chemicals was statistically compared at each time point, for each model, by ANOVA with Tukey's test. 'a' denotes $p < 0.05$ when comparing caffeine and salicylic acid; 'b' denotes $p < 0.05$ when comparing caffeine and testosterone; 'c' denotes $p < 0.05$ when comparing salicylic acid and testosterone. All other comparisons were determined to be not statistically significant. Mass distribution values were adjusted using an arcsin-square root transformation and chemicals within collection groups (i.e., donor, tissue, or receptor) were compared by ANOVA with Tukey's test. * = $p < 0.05$, ** = $p < 0.01$, *** = $p < 0.001$. All other comparisons were determined to be not statistically significant.
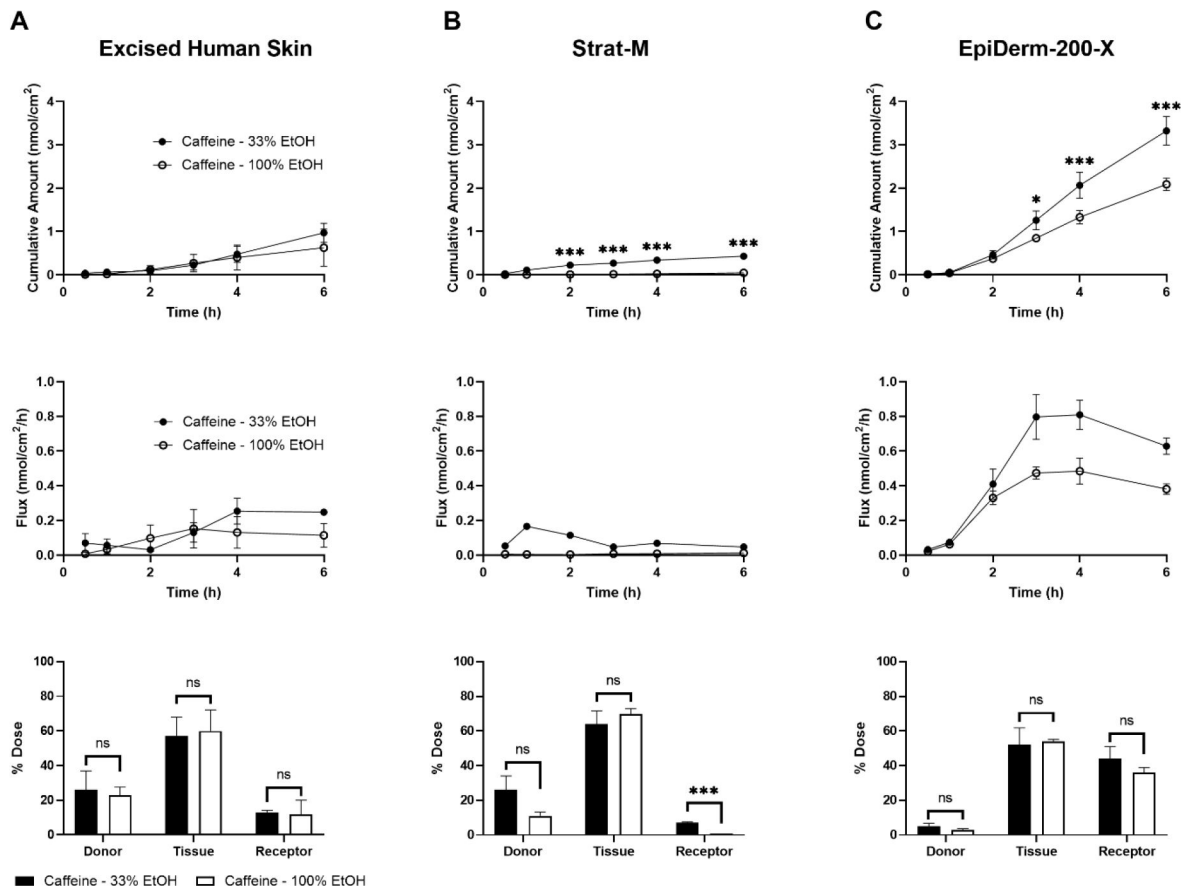
Figure 5.

Evaluation of the vehicle effect on permeation of caffeine (Log K_{ow} = −0.07) through excised human skin (EHS) (A), Strat-M (B), and EpiDerm-200-X (C). EHS and alternative skin barrier models were mounted on 5 mm Franz cells and a finite dose of caffeine (6 nmol/cm^2; 10 μL/cm^2) in 33% or 100% ethanol (EtOH) was applied topically. Cumulative amount permeated (top row), flux (middle row), and mass distribution (bottom row) were determined over 6 h. N = 3 donors/batches per barrier for each formulation, each in triplicate. Data shown as mean ± standard error of mean. Mean cumulative amount across vehicles was statistically compared at each time point, for each model, by ANOVA with the maximum modulus test. * = $p < 0.05$, *** = $p < 0.001$. Mass distribution values were adjusted using an arcsin-square root transformation and chemicals within collection groups (i.e., donor, tissue, or receptor) were compared by ANOVA with the maximum modulus test. ns = no significance, *** = $p < 0.001$.
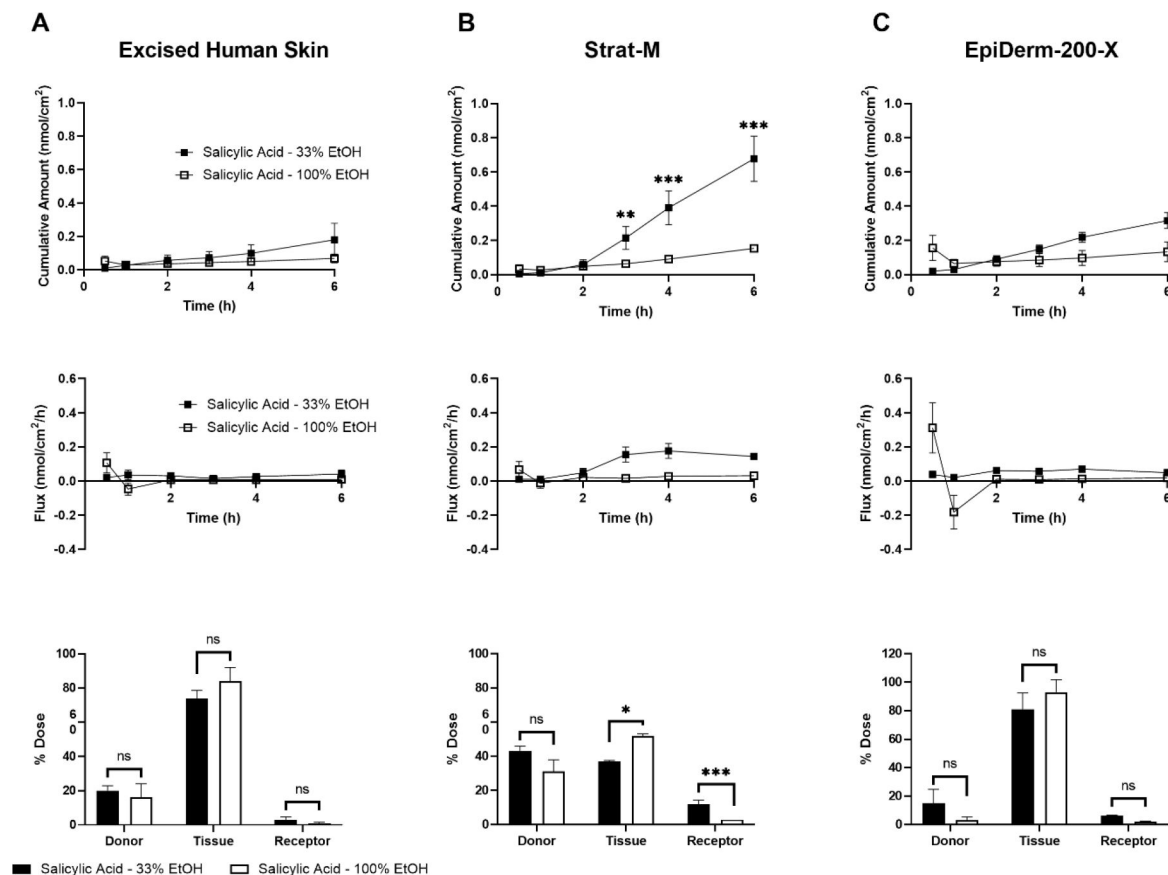
Figure 6.

Evaluating vehicle influence on permeation of salicylic acid (Log K_{ow} = 2.26) through excised human skin (EHS) (A), Strat-M (B), and EpiDerm-200-X (C). EHS and alternative skin barrier models were mounted on 5 mm Franz cells and a finite dose of salicylic acid (6 nmol/cm^2; 10 μL/cm^2) in 33% or 100% ethanol (EtOH) was applied topically. Cumulative amount permeated (top row), flux (middle row), and mass distribution (bottom row) were determined over 6 h. N = 3 donors/batches per barrier for each formulation, each in triplicate. Data shown as mean ± standard error of mean. Mean cumulative amount across vehicles was statistically compared at each time point, for each model, by ANOVA with the maximum modulus test. ** = $p < 0.01$, *** = $p < 0.001$. Mass balance values were adjusted using an arcsin-square root transformation and chemicals within collection groups (i.e., donor, tissue, or receptor) were compared by ANOVA with the maximum modulus test. ns = no significance, * = $p < 0.05$, *** = $p < 0.001$.

Table 1.

Summary of 6 h cumulative permeations (mean ± standard error of mean) and statistical analyses (*p*-value). N = 3 donors/batches, each in triplicate.

Barrier	6 h Cumulative Permeation (nmol/cm^2)			Statistical Analysis (*p*-value)		
	Caffeine	Salicylic acid	Testosterone	Caffeine vs salicylic acid	Caffeine vs testosterone	Salicylic acid vs testosterone
Excised Human Skin (EHS)	0.97 ± 0.22	0.18 ± 0.10	0.33 ± 0.13	**< 0.001**	**< 0.001**	0.701
Strat-M	0.43 ± 0.03	0.68 ± 0.13	0.05 ± 0.03	0.292	**0.043**	**< 0.001**
EpiDerm-200-X	3.32 ± 0.33	0.32 ± 0.05	2.99 ± 0.31	**< 0.001**	0.086	**< 0.001**

	Statistical Analysis (*p*-value)		
EHS vs Strat-M	**0.002**	**0.005**	0.195
EHS vs EpiDerm-200-X	**< 0.001**	0.760	**< 0.001**
Strat-M vs EpiDerm-200-X	**< 0.001**	0.058	**< 0.001**